



Deep-blue phosphorescent iridium complexes with picolinic acid N-oxide as the ancillary ligand for high efficiency organic light-emitting diodes

Hoe-Joo Seo ^{a,1}, Kyung-Mo Yoo ^{b,1}, Myungkwan Song ^c, Jin Su Park ^c, Sung-Ho Jin ^c,
Young Inn Kim ^{c,*}, Jang-Joo Kim ^{b,*}

^a Department of Chemistry and Center for Plastic Information System, Pusan National University, Busan 609-735, Republic of Korea

^b Department of Materials Science and Engineering and OLED Center, Seoul National University, Seoul 151-744, Republic of Korea

^c Department of Chemistry Education, Interdisciplinary Program of Advanced Information and Display Materials, Center for Plastic Information System, Pusan National University, Busan 609-735, Republic of Korea

ARTICLE INFO

Article history:

Received 30 October 2009

Received in revised form 19 December 2009

Accepted 19 December 2009

Available online 29 December 2009

Keywords:

Phosphorescent organic light-emitting diodes (PhOLEDs)

Iridium complex

Deep-blue emitter

External quantum efficiency

Picolinic acid N-oxide ancillary ligand

ABSTRACT

A new series of highly efficient deep-blue phosphorescent Ir(III) complexes, (F₂CH₃ppy)₂Ir(pic-N-oxide) **6** and (F₂CF₃CH₃ppy)₂Ir(pic-N-oxide) **7**, based on phenylpyridine (ppy) as the main ligand and picolinic acid N-oxide (pic-N-oxide) as the ancillary ligand, were synthesized for applications in phosphorescent organic light-emitting diodes (PhOLEDs). The photophysical, electrochemical, and electroluminescent (EL) properties of these substances were investigated. The energy levels of these substances were adjusted by the introduction of electron-donating and electron-withdrawing substituents on the ppy ligand. The Ir(III) complexes have high phosphorescent quantum yields as well as high thermal stability. High performance PhOLEDs fabricated using the Ir(III) complexes showed bright deep-blue emissions with the Commission Internationale de L'Eclairage (CIE) coordinates of (0.147, 0.210) at the current density of 0.1 mA/cm², and high external quantum (23.3%) and current (36.1 cd/A) efficiencies.

© 2009 Elsevier B.V. All rights reserved.

1. Introduction

Organic light-emitting diodes (OLEDs) are currently attracting great attention owing to their potential applications in full-color flat panel displays that serve as an efficient and low cost alternative to the widely used liquid crystal displays. An intense effort has been devoted to developing emitting materials and device structures for OLEDs in order to obtain higher efficiencies that are required for commercialization [1–4]. For commercial full-color OLEDs, materials that emit in the three basic color regions of blue, green, and red are required. Blue emitting materials are not only one of the major constituents

in red-green-blue full-color displays, they also serve as the key emitting element for generating white light in combination with a complementary yellow color. As a result, explorations for new blue emitting materials that have higher performances remains one of the major challenges in this field.

Heavy-metal complexes, particularly those containing Ir(III), have been employed successfully in the construction of high efficiency phosphorescent organic light-emitting diodes (PhOLEDs) in displays and solid-state lighting [5–16]. In these systems, both triplet and singlet excitons are harvested as light by doping the phosphorescent emitters into charge-transporting hosts. Close to 100% internal quantum efficiencies have been reported for Ir(III) complexes in PhOLEDs [17–20]. Deep-blue Ir(III) complexes are needed in order to effectively reduce power consumption and increase the color gamut of full-color OLEDs. Importantly, the emission wavelengths of these complexes

* Corresponding authors.

E-mail addresses: yikim@pusan.ac.kr (Y.I. Kim), jjkim@snu.ac.kr (J.-J. Kim).

¹ H.J. Seo and K.M. Yoo made equal contribution to this paper.

can be readily tuned from red/green to sky blue by modification of the metal ligands. For example, emission from Ir(III) complexes can cover the whole visible region by simply modifying the 2-arylpyridine main ligand and the ancillary ligand [21]. However, in contrast to green and red phosphorescent complexes, the design and synthesis of deep-blue emitting Ir(III) complexes is a more challenging task [22–29].

Two strategies exist for creating phosphorescent Ir(III) complexes whose deep-blue emission is governed by the energy difference between the highest occupied molecular orbital (HOMO) and lowest unoccupied molecular orbital (LUMO). The first involves low-lying the energy of the HOMO of the Ir(III) complexes [30–36]. 2-(2,4-Difluorophenyl)pyridine based Ir(III) complexes are good examples of the implementation of this strategy. In these types of Ir(III) complexes, electron-withdrawing fluorines are introduced on the phenyl ring to cause a high HOMO energy. The second method relies on an high-lying the energy of the LUMO. This strategy has been used in the design of *fac*-Ir(F₂MeOppy)₃ [F₂MeOppy: 2-(2',4'-difluorophenyl)-4-methoxypyridinato] and (F₂MeOppy)₂Ir(ptz) [ptz: 5-(2-pyridyl)tetrazolate], which emit at 464 nm [31] and 452 nm [37], respectively. The blue shift seen in these substances is ascribed to the effect of the strong electron-donating substituents at the 4-position of the pyridyl moiety low LUMO energy level. Several groups have demonstrated that phosphorescent wavelengths can be tuned in the blue to red region by functionalization of the main ligands of Ir-complexes with electron-withdrawing and electron-donating substituents [38–41].

Another important requirement for PhOLED applications is that the Ir(III) complexes have high phosphorescent quantum efficiencies. The physical properties, such as charge transfer character and solubility, of the Ir(III) complexes in heteroleptic Ir(III) complexes can be regulated through a proper choice of the ancillary ligand. Also, the nature of the ancillary ligand can profoundly effect the properties of lowest energy emitting excited state of the complex [42,43]. The electron density at the metal center can be controlled by the electron-donating or electron-withdrawing character of the ancillary ligand. The ground state electron density at the metal center governs the amount of metal to ligand charge transfer (MLCT) character that is mixed into the lowest energy electronic transition and, consequently, it governs both the emission wavelength and excited state radiative lifetime.

Despite the fact that significant work has been carried out in this area, efficient and stable deep-blue Ir(III) complexes are still rare. As a result, the design and synthesis of high performance, deep-blue Ir(III) complexes is a subject of great continuing [44,45]. Below, we describe the synthesis and properties of novel deep-blue emitting Ir(III) complexes **6** and **7** that have been designed by using the two strategies discussed above. Importantly, picolinic acid N-oxide (pic-N-oxide) is used for the first time in these complexes as the ancillary ligand. In addition, the complexes contain a methyl group at the 4-position of the pyridyl ring of the 2-(2,4-difluorophenyl)pyridine ligand **1** and the 2-(2',4'-difluoro-3'-trifluoromethylphenyl)-4-methylpyridine ligand **3**. The combination of

these substituents promotes an increase in the HOMO–LUMO energy gap, resulting in a hypsochromic shift compared to emission from the parent Ir(III) complex. PhOLEDs fabricated using these deep-blue Ir(III) complexes exhibit a maximum external quantum efficiency of 23.3% and deep-blue emission with the Commission Internationale de l'Éclairage (CIE) coordinates of (0.147, 0.210). To our best knowledge, the quantum efficiency is the highest among PhOLEDs emitting deep-blue color with the y value close to 0.2 in the CIE coordinate.

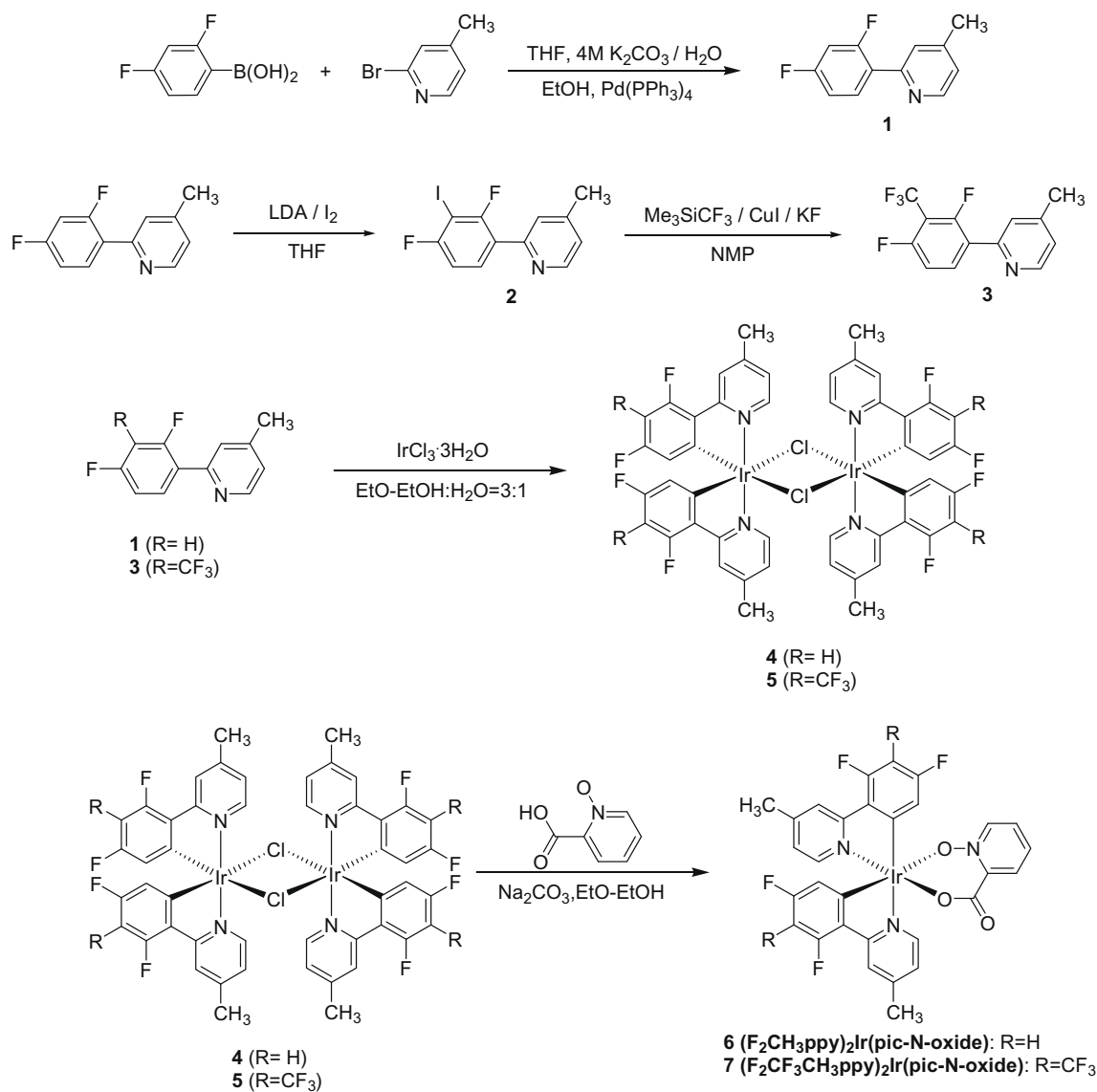
2. Results and discussion

The deep-blue emitting Ir(III) complexes (F₂CH₃ppy)₂-Ir(pic-N-oxide) **6** and (F₂CF₃CH₃ppy)₂Ir(pic-N-oxide) **7** (Scheme 1) were designed on the basis of considerations that include the ability to tune (1) HOMO–LUMO energy gaps by introduction of electron-donating and electron-withdrawing substituents into the phenylpyridine main ligand, and (2) electro-optical properties for enhanced PhOLED performance by modify the ancillary ligand. As a result, the target Ir(III) complexes **6** and **7** contain difluoro or difluoro and a trifluoromethyl group substituents on the phenyl group of the 2-phenyl-4-methylpyridine main ligand and pic-N-oxide as the ancillary ligand.

The procedure used to prepare the target Ir(III) complexes **6** and **7** involves coupling of IrCl₃·3H₂O with the main ppy ligand followed by introduction of the ancillary pic-N-oxide ligand (Scheme 1) [46]. In order to prepare the main ligand **3**, 2-(2',4'-difluorophenyl)-4-methylpyridine (**1**, Fig. S1), prepared in 83% yield by employing a Suzuki coupling reaction between 2,4-difluorophenylboronic acid and 2-bromo-4-methylpyridine, was transformed to the iodo derivative **2** (Fig. S2) in 76% yield by sequential treatment with LDA and iodine. Reaction of **2** with (trifluoromethyl)trimethylsilane in the presence of CuI and KF gave 2-(2',4'-difluoro-3'-trifluoromethylphenyl)-4-methylpyridine (**3**, Fig. S3) in 39% yield.

The cyclometalated Ir(III) μ -chloride bridged dimeric ((C^N)₂Ir(μ -Cl))₂ complexes **4** and **5** were independently synthesized by reacting IrCl₃·3H₂O with an excess of the respective main ligands 2-(2',4'-difluorophenyl)-4-methylphenylpyridine (**1**) and 2-(2',4'-difluoro-3'-trifluoromethylphenyl)-4-methylpyridine (**3**) in 79–86% yields. Finally, replacement of the two bridging chlorides in **4** and **5** with pic-N-oxide produces the desired complexes (F₂CH₃ppy)₂-Ir(pic-N-oxide) **6** and (F₂CF₃CH₃ppy)₂Ir(pic-N-oxide) **7** in yields of ca. 50%. Ir(III) complexes **6** and **7** were purified by using silica gel column chromatography followed by multiple sublimation with a high vacuum, gradient temperature train sublimation procedure. The structures, purities, and properties of the Ir(III) complexes **6** and **7** were determined by using ¹H NMR spectroscopy (Figs. S4 and S5), elemental analysis, differential scanning calorimetry (DSC), thermal gravimetric analysis (TGA), CV, UV–visible, and PL spectroscopy.

The thermal stabilities of the Ir(III) complexes **6** and **7** were evaluated using TGA and DSC under a nitrogen atmosphere. The 5% weight loss temperatures ($\Delta T_{5\%}$), recorded in Table 1, indicate that (F₂CH₃ppy)₂Ir(pic-N-oxide) **6** and



Scheme 1. Synthesis of Ir(III) complexes **6** and **7**.

Table 1

Thermal and photophysical property of Ir(III) complexes.

Complex	T_g [°C] ^a	T_d [°C] ^b	λ_{max} [nm] ^c	HOMO [eV] ^d	LUMO [eV] ^e	τ [μs] ^f	η_{PL} [%] ^g
(F ₂ CH ₃ ppy) ₂ Ir(pic-N-oxide)	165	346	463, 491	-5.9	-3.0	1.46	67 ± 5
(F ₂ CF ₃ CH ₃ ppy) ₂ Ir(pic-N-oxide)	216	377	454, 482	-6.2	-3.2	1.48	80 ± 5

^a T_g : glass transition temperature.

^b T_d : decomposition temperature.

^c λ_{max} : wavelengths of photoluminescence peaks.

^d HOMO: highest occupied molecular orbital energy levels referenced to vacuum level.

^e LUMO: lowest unoccupied molecular orbital energy levels referenced to vacuum level.

^f τ : exciton lifetime when doped with 6 wt% in mCP film.

^g η_{PL} : PL efficiency when doped with 6 wt% in mCP film.

(F₂CF₃CH₃ppy)₂Ir(pic-N-oxide) **7** have excellent thermal stabilities of 346 °C and 377 °C, since picolinic acid N-oxide ligand formed thermodynamically stable six membered

ring with Ir(III) metal ion. The observations indicate that the Ir(III) complexes **6** and **7** have enhanced the rigidities that should prevent degradation of emitting layers of

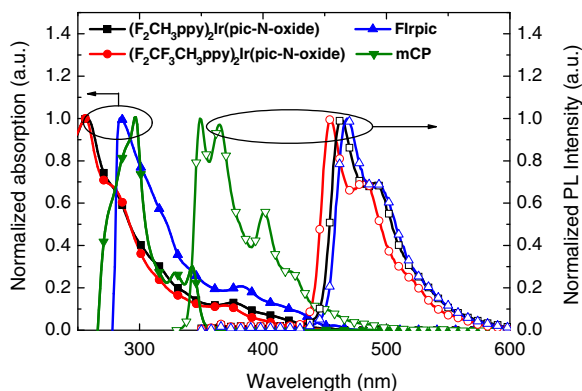


Fig. 1. Normalized absorption spectra (closed symbols) and PL spectra (open symbols) of $(F_2CH_3ppy)_2Ir(pic-N-oxide)$ **6** (square), $(F_2CF_3CH_3ppy)_2Ir(pic-N-oxide)$ **7** (circle), Flrpic (up triangle), and mCP (down triangle).

PhOLEDs caused by the current-induced heat. The glass transition temperatures of Ir(III) complexes **6** and **7** are 165 and 216 °C, respectively. Importantly, the blue Ir(III) complex **7** that contains the trifluoromethyl substituent exhibits a higher thermal stability than the Ir(III) complex **6** which lacks this substituent.

The absorption spectra of the Ir(III) complexes $(F_2CH_3ppy)_2Ir(pic-N-oxide)$ **6** and $(F_2CF_3CH_3ppy)_2Ir(pic-N-oxide)$ **7** as well as Flrpic in dilute solutions (*ca.* 10^{-5} M in dichloromethane) and the absorption spectrum of mCP in film states are shown in Fig. 1 along with the PL spectra of the Ir(III) complexes and mCP. As is commonly seen with most Ir(III) complexes, the absorption spectra of these Ir(III) complexes **6** and **7** can be divided into two regions [47,48]. The intense peaks in the short wavelength regions below 400 nm are assigned to spin-allowed $^1\pi-\pi^*$ transitions that closely resemble those present in spectra of ppy main ligands (λ_{max} : 273 nm). The weaker absorption shoulders that appear above 400 nm are associated with charge transfer transitions [49]. The data suggest that substantial mixing takes place between ligand-based $^3\pi-\pi^*$ states, spin forbidden metal to ligand charge transfer (3MLCT) states, and higher-lying 1MLCT transition states induced by the spin-orbit coupling effect [50,51]. The spin-orbit coupling is enhanced by the presence of closely-spaced $\pi-\pi^*$ and MLCT states and the heavy-atom effect of Ir(III) center [52,53].

PL spectra were obtained on doped films of the Ir(III) complexes **6** and **7** in mCP with the concentrations of 8 wt.%. Optical band gaps of Ir(III) complexes **6** and **7**, deduced from the absorption edge of the absorption spectra, are 2.92 eV and 3.00 eV, respectively, both of which are larger than that of Flrpic (2.90 eV). The Ir(III) complexes **6** and **7** were found to emit intense deep-blue light, as shown in Fig. 1. The $(F_2CH_3ppy)_2Ir(pic-N-oxide)$ **6** and $(F_2CF_3CH_3ppy)_2Ir(pic-N-oxide)$ **7** complexes exhibit maximum PL peaks at 463 nm and 454 nm, deriving predominantly from ligand-centered $^3\pi-\pi^*$ excited states, that are blue shifted from the maximum peak of 468 nm arising from Flrpic. Triplet energy levels (T_1) are 2.65 eV for Flrpic, 2.68 eV for $(F_2CH_3ppy)_2Ir(pic-N-oxide)$ **6**, and 2.73 eV for $(F_2CF_3CH_3ppy)_2Ir(pic-N-oxide)$ **7**, respectively.

The PL efficiencies of mCP films doped with the Ir(III) complexes were determined using an integrating sphere with a He:Cd laser (λ : 325 nm and continuous wave) as the excitation light source. $(F_2CF_3CH_3ppy)_2Ir(pic-N-oxide)$ **7** exhibits a very large PL quantum efficiency of $80 \pm 5\%$, which is almost the same as Flrpic ($87 \pm 3\%$). In contrast, $(F_2CH_3ppy)_2Ir(pic-N-oxide)$ **6** has a slightly lower PL efficiency of $67 \pm 5\%$.

The transient PLs of the Ir(III) complexes, doped in mCP at a concentration of 6 wt.%, display single exponential decays, indicating that the bi-molecular interactions are negligible at this concentration (Fig. S6). Exciton lifetimes of the Ir(III) complexes were determined to be 1.46 μ s and 1.48 μ s for $(F_2CH_3ppy)_2Ir(pic-N-oxide)$ **6** and $(F_2CF_3CH_3ppy)_2Ir(pic-N-oxide)$ **7**, respectively, values that are comparable to that of Flrpic (1.43 μ s). The HOMO energy levels of the Ir(III) complexes, obtained by using CV measurements, are -5.9 eV for $(F_2ppy)_2Ir(pic-N-oxide)$ **6** and -6.2 eV for $(F_2CF_3CH_3ppy)_2Ir(pic-N-oxide)$ **7**. Both CVs are reversible and stable over repeated scans, implying that the Ir(III) complexes are stable under the oxidation conditions. By combining HOMO energy and optical band gap measurements, LUMO energy levels of -3.0 eV and -3.2 eV were determined for $(F_2CH_3ppy)_2Ir(pic-N-oxide)$ **6** and $(F_2CF_3CH_3ppy)_2Ir(pic-N-oxide)$ **7**, respectively. The higher electron density on the oxygen atom of N-oxide in pyridyl ring is expected to increase the energy level of LUMO and consequently results in a blue-shifted emission. Although the higher energy level of LUMO from the $(F_2CH_3ppy)_2Ir(pic-N-oxide)$ **6** was observed, compared to that of Flrpic, the electron-withdrawing CF_3 -group in $(F_2CF_3CH_3ppy)_2Ir(pic-N-oxide)$ **7** makes both energy levels of HOMO and LUMO lower. This is primarily responsible for the blue-shift of an emission peak. The energy levels and the photophysical data for $(F_2CH_3ppy)_2Ir(pic-N-oxide)$ **6** and $(F_2CF_3CH_3ppy)_2Ir(pic-N-oxide)$ **7** are summarized in Table 1.

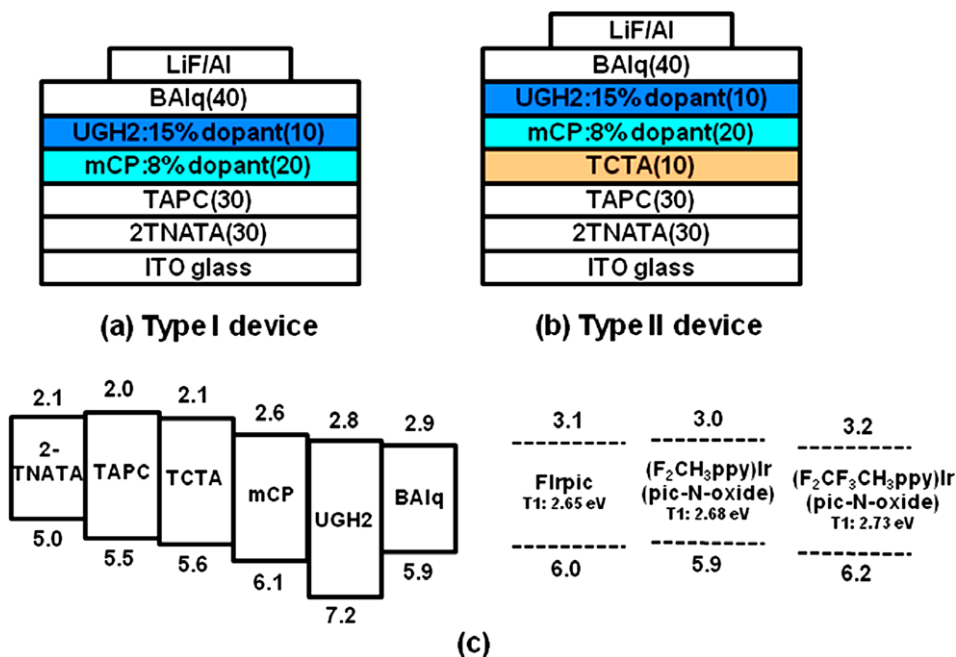
PhOLEDs were fabricated using the Ir(III) complexes **6** and **7** as dopants in mCP, selected as the host material because of its large spectral overlap with Ir(III) complexes **6** and **7** (Fig. 1) and higher triplet energy level than the Ir(III) complexes **6** and **7**. PhOLED with Flrpic as a dopant were also fabricated for comparison purposes. The PhOLEDs performance of these Ir(III) complexes **6**, **7**, and Flrpic are summarized in Table 2.

In Fig. 2 is shown the structures of the PhOLEDs and the energy levels of the compounds used in this study. The Type I PhOLEDs, fabricated on a clean glass substrate precoated with indium tin oxide (ITO), have the following components: ITO/4,4',4''-tris(N-(2-naphthyl)-N-phenylamino)triphenylamine (2-TNATA) as a hole transporting layer (30 nm)/1,1-bis[(di-4-tolylamino)phenyl]cyclohexane (TAPC) (30 nm) as an electron blocking layer/mCP:8 wt.% dopant (20 nm)/*p*-bis(triphenylsilyl)benzene (UGH2):15 wt.% dopant (10 nm)/aluminium(III) bis(2-methyl-8-quinolate)-4-phenylphenolate (BALq) (40 nm) as the electron transporting layer/LiF (1 nm)/Al (100 nm). The PhOLEDs have dual emission layers in order to bring about a better balance between the electron and hole. mCP and UGH2 were selected as the *p*-host and the *n*-host, respectively. mCP has a large spectral overlap with Ir(III)

Table 2

EL performance of Ir(III) complexes.

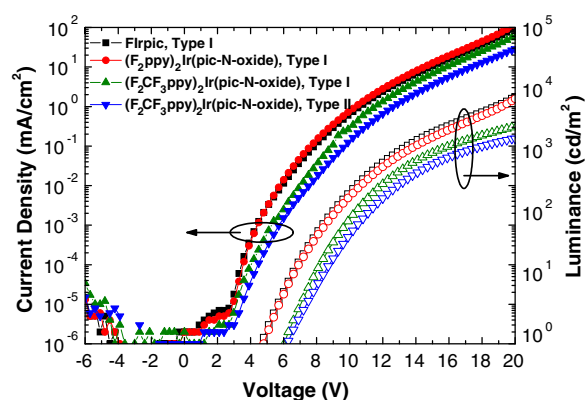
Type	EML	EQE [%] ^a	CE [cd/A] ^a	PE [lm/W] ^a	CIE [x, y] ^b	EQE [%] ^c	LE [cd/A] ^c	PE [lm/W] ^c	CIE [x, y] ^c
I	Flrpic	22.6	42.8	27.5	0.151, 0.307	7.1	14.1	2.7	0.158, 0.322
I	(F ₂ CH ₃ ppy) ₂ Ir(pic-N-oxide)	19.6	34.5	22.6	0.161, 0.278	5.7	10.8	2.1	0.168, 0.291
I	(F ₂ CF ₃ CH ₃ ppy) ₂ Ir(pic-N-oxide)	21.4	31.6	14.3	0.149, 0.193	5.3	8.0	1.5	0.153, 0.200
II	(F ₂ CF ₃ CH ₃ ppy) ₂ Ir(pic-N-oxide)	23.3	36.1	17.3	0.147, 0.210	4.2	6.7	1.1	0.152, 0.221

^a Maximum efficiency.^b Values collected at a current density of 0.1 mA/cm².^c Values collected at a current density of 20 mA/cm².**Fig. 2.** Structures of the devices for (a) Type I and (b) Type II, and (c) energy levels of materials used in the study.

complexes **6** and **7** (Fig. 1) and as a result, it should promote efficient energy transfer. Both of the hosts have higher triplet energy levels than the Ir(III) complexes **6** and **7** in order to block triplet energy transfer from the Ir(III) complexes **6** and **7** to the hosts. UGH2 also works as an electron transport and exciton blocking layer. Concentrations of the Ir(III) complexes **6** and **7** were selected to be 8 wt.% in mCP and 15 wt.% in UGH2, respectively, which give optimal performances of the PhOLEDs.

Another type of (F₂CF₃CH₃ppy)₂Ir(pic-N-oxide) **7** derived PhOLED (Type II) was fabricated by adding a TCTA layer in an attempt to reduce accumulation of holes at HTL/EML interface. This PhOLED that has the following components: ITO/2-TNATA (30 nm)/TAPC (30 nm)/TCTA (10 nm)/mCP:8 wt.% **7** (20 nm)/UGH2:15 wt.% (F₂CF₃CH₃ppy)₂Ir(pic-N-oxide) (10 nm)/BAlq (40 nm)/LiF (1 nm)/Al (100 nm).

As shown in Fig. 3, current density–voltage–luminance curves (*J–V–L*) of the PhOLEDs prepared from Flrpic and (F₂CH₃ppy)₂Ir(pic-N-oxide) **6** are almost the same, indicating that the small energy differences in the HOMO and LUMO energy levels of the Ir(III) complexes **6** and **7** have little effect on charge transport. The turn-on voltage is

**Fig. 3.** Current density–voltage–luminance characteristics of the devices.

slightly high (4.5 V) owing to the high injection barrier of holes from TAPC and low electron mobility in UGH2. The PhOLED doped with (F₂CF₃CH₃ppy)₂Ir(pic-N-oxide) **7** require a slightly higher driving voltage than those studied

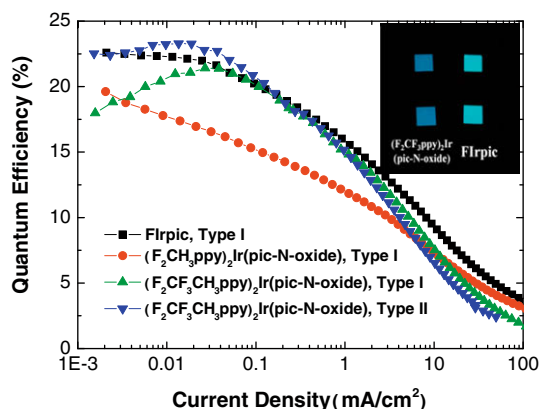


Fig. 4. External quantum efficiency of the devices. Inset: images of $(F_2CF_3CH_3ppy)_2Ir(pic-N-oxide)$ **7** devices and Flrpic devices.

previously most likely caused by the low HOMO and LUMO energy levels of the Ir(III) complexes **6** and **7**.

External quantum efficiencies of the PhOLEDs are displayed in Fig. 4. The Type I PhOLED doped with $(F_2CF_3CH_3ppy)_2Ir(pic-N-oxide)$ **7** as the emitter has the very large maximum external quantum efficiency of 21.4%, which is very close to the reference Flrpic. Insertion of a 10 nm thick TCTA layer between the TAPC and mCP/ $(F_2CF_3CH_3ppy)_2Ir(pic-N-oxide)$ layers in the Type II device results in the even larger maximum external quantum efficiency of 23.3%.

The EL spectra of the PhOLEDs, especially at the low current density of 0.1 mA/cm^2 , are the same as the solution PL spectra of the Ir(III) complexes **6** and **7**, displaying deep-blue emissions with Commission Internationale de l'Eclairage (CIE) coordinates of (0.149, 0.193) for the Type I and (0.147, 0.210) for the Type II devices, compared to a Type I device with Flrpic (0.151, 0.307) (Fig. S7). The emission color of the $(F_2CF_3CH_3ppy)_2Ir(pic-N-oxide)$ **7** based PhOLED is compared with the Flrpic based PhOLED in the inset in Fig. 4, clearly displaying deep-blue color. The observed efficiencies and deep-blue emission demonstrate that these PhOLEDs have the best performance of any blue PhOLEDs studied to date with the y value close to 0.2 in the CIE coordinate. The PhOLEDs doped with $(F_2CH_3ppy)_2Ir(pic-N-oxide)$ **6** have a slightly lower maximum external quantum efficiency (19.6%) as a consequence of the lower PL quantum efficiency. The CIE coordinate of the $(F_2CH_3ppy)_2Ir(pic-N-oxide)$ based PhOLED is (0.161, 0.278) at the current density of 0.1 mA/cm^2 . All the PhOLEDs made using $(F_2CF_3CH_3ppy)_2Ir(pic-N-oxide)$ **7** showed better performance for the Devices II structure than the Devices I, as listed in Table 2.

All the PhOLEDs prepared in this investigation show a large roll-off efficiencies with increasing current, which likely originates from a shift of the recombination zone as well as triplet-triplet and triplet-polaron annihilation at high current density [54]. The hypothesized existence of a recombination zone shift is supported by the observed variation of the emission spectra of the PhOLEDs with current density. The intensity ratios of the two vibronic peaks in the EL spectra of the dopants of $(F_2CF_3CH_3ppy)_2Ir(pic-N-oxide)$

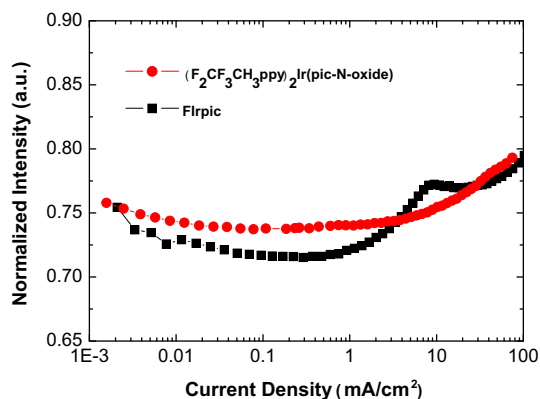


Fig. 5. Variation of relative peak intensity of longer wavelength vibronic peak to that of shortwavelength vibronic peak in EL spectra with increasing current.

7 ($I_{482 \text{ nm}}/I_{454 \text{ nm}}$) and Flrpic ($I_{491 \text{ nm}}/I_{463 \text{ nm}}$) are displayed in Fig. 5. The ratios increase with increasing current density above 1 mA/cm^2 for both PhOLEDs. The increasing ratio, associated with an intensified emission of the long wavelength vibronic peak with increasing current, suggests that the recombination zone shifts away from the Al electrode with increasing current. This roll-off can be minimized by a proper choice of electron and hole transporting, and host materials, as demonstrated for the Flrpic doped PhOLEDs.

3. Conclusions

Deep-blue emitting Ir(III) complexes containing electron density modulated phenylpyridine main ligands and a pic-N-oxide ancillary ligand have been synthesized. The new Ir(III) complexes are thermally and electrochemically stable and they have high photoluminescence efficiencies of over 80%. PhOLEDs fabricated using these Ir(III) complexes showed high external quantum (23.3%), current efficiencies (36.1 cd/A) and deep-blue emission with a CIE coordinate of (0.147, 0.210). Owing to these important characteristics, PhOLEDs prepared from these deep-blue Ir(III) complexes hold high potential for applications in display and solid-state lighting technologies.

4. Experimental

4.1. General information

All reagents and solvents were purchased from Aldrich Chemical Co., Fluka and Alfa Aesar, and used without further purification. Anhydrous tetrahydrofuran (THF) was distilled over sodium and benzophenone under a nitrogen atmosphere. Silica column chromatography was performed using silica gel 60 G (particle size 5–40 μm , Merck Co.).

4.2. Synthesis of 2-(2',4'-difluorophenyl)-4-methylpyridine (1)

2-(2',4'-Difluorophenyl)-4-methylpyridine (**1**) was prepared by using a Suzuki coupling reaction between 2,4-difluorophenylboronic acid and 2-bromo-4-methylpyridine

[55]. 2-Bromo-4-methylpyridine (2.54 g, 20 mmol) and 2,4-difluorophenylboronic acid (3.47 g, 22 mmol) were dissolved in freshly distilled THF (100 mL) under nitrogen atmosphere. Potassium carbonate in water (10 mL, 2 M) and ethanol (2 mL) were added and the resulting mixture was cooled in a liquid nitrogen bath and thoroughly degassed. Tetrakis(triphenylphosphine)palladium(0) (1.2 g, 1 mmol) was added and the resulting mixture stirred at 70 °C for 24 h, cooled to room temperature, poured into water (100 mL), and extracted with diethyl ether (50 mL \times 3 times). The combined organic layers were washed with water (50 mL) and brine (50 mL), dried over anhydrous magnesium sulfate, and concentrated *in vacuo* giving a residue, which was subjected to flash chromatography on silica gel using *n*-hexane/ethyl acetate as the eluent to yield **1** (3.41 g, 83%). $^1\text{H NMR}$ (300 MHz, CDCl_3 , ppm): 8.55 (d, 1H, $J = 4.8$ Hz), 7.94 (td, 1H, $J = 6.6, 10.5$ Hz), 7.55 (s, 1H), 7.08 (d, 1H, $J = 4.5$ Hz), 6.89–7.01 (m, 2H), 2.41 (s, 3H).

4.3. Synthesis of 2-(2',4'-difluoro-3'-iodophenyl)-4-methylpyridine (**2**)

2-(2',4'-Difluoro-3'-iodophenyl)-4-methylpyridine (**2**) was prepared by using the published procedure [56]. 2-(2',4'-Difluorophenyl)-4-methylpyridine (3.41 g, 16.6 mmol) was dissolved in freshly distilled THF (50 mL) under a nitrogen atmosphere. Lithium diisopropylamide (10 mL, 2 M) in *n*-hexane/THF was added dropwise to the solution at -78 °C and the mixture was stirred for 1 h. A solution of iodine (4.64 g, 18.3 mmol) in THF (20 mL) was added and the mixture was stirred for 3 h at -78 °C, warmed to room temperature, and poured into water (50 mL). The combined organic layers obtained by extraction with diethyl ether (50 mL \times 3 times) was washed with saturated sodium thiosulfate (50 mL) and brine (50 mL), dried over anhydrous magnesium sulfate and concentrated *in vacuo* giving a residue which was subjected to flash chromatography on silica gel using *n*-hexane/ethyl acetate as the eluent to give **2** (4.18 g, 76%). $^1\text{H NMR}$ (300 MHz, CDCl_3 , ppm): 8.57 (d, 1H, $J = 4.8$ Hz), 7.95 (td, 1H, $J = 6.3, 8.7$ Hz), 7.57 (s, 1H), 7.13 (d, 1H, $J = 4.8$ Hz), 6.99–7.05 (m, 1H), 2.42 (s, 3H).

4.4. Synthesis of 2-(2',4'-difluoro-3'-trifluoromethylphenyl)-4-methylpyridine (**3**)

2-(2',4'-Difluoro-3'-trifluoromethylphenyl)-4-methylpyridine (**3**) was prepared by using the published procedure [56]. A mixture of copper(I) iodide (6.00 g, 31.5 mmol) and anhydrous potassium fluoride (1.10 g, 19.0 mmol) was heated under reduced pressure while being gently shaken until the color changed to yellow. 2-(2',4'-Difluoro-3'-iodophenyl)-4-methylpyridine (4.18 g, 12.6 mmol), 1-methyl-2-pyrrolidone (30 mL), and (trifluoromethyl)trimethylsilane (4 mL) were added to the mixture which was then vigorously stirred for 24 h at room temperature. The mixture was poured into aqueous ammonia (14%, 100 mL) and extracted with dichloromethane (50 mL \times 3 times) to give an organic phase that was washed with water (50 mL) and brine (50 mL), dried over anhydrous magnesium sulfate and concentrated *in vacuo*.

The residue was subjected to flash chromatography on silica gel using *n*-hexane/ethyl acetate as the eluent to give **3** (1.39 g, 39%). $^1\text{H NMR}$ (300 MHz, CDCl_3 , ppm): 8.59 (d, 1H, $J = 5.1$ Hz), 7.98 (td, 1H, $J = 6.3, 9$ Hz), 7.60 (s, 1H), 7.17 (d, 1H, $J = 4.8$ Hz), 7.01–7.07 (m, 1H), 2.46 (s, 3H).

4.5. General procedure for the synthesis of $(C^{\wedge}N)_2\text{Ir}(\text{pic-N-oxide})$ complexes **6** and **7**

The $(C^{\wedge}N)_2\text{Ir}(\text{pic-N-oxide})$ complexes were synthesized in two steps using standard method [5,57]. A solution of $\text{IrCl}_3 \cdot 3\text{H}_2\text{O}$ (0.70 g, 2 mmol) and 2.5 equivalents of the main ligand **1** or **3** in 2-ethoxyethanol/water (16 mL, 3:1 v/v) was stirred at 125 °C for 24 h, cooled to room temperature, and concentrated *in vacuo*. Washing the residue with ethanol gave rise to the dimeric iridium complexes $[(C^{\wedge}N)_2\text{Ir}(\mu\text{-Cl})_2]$ **4** or **5**. After drying, the crude product was directly used for next step without further purification. A solution of either **4** or **5** (1 mmol), Na_2CO_3 (10 mmol) and 5 equivalents of pic-N-oxide in 2-ethoxyethanol (10 mL) was stirred at 130 °C under a nitrogen atmosphere for 20 h, cooled, and poured into water. Extraction with dichloromethane (30 mL \times 3 times) gave an organic layer which was dried over anhydrous magnesium sulfate, and concentrated *in vacuo* giving a residue that was subjected to flash chromatography on silica gel using dichloromethane/methanol as the eluent to afford the desired Ir(III) complexes **6** and **7**, respectively.

4.5.1. Dimer iridium complex **4**

Tetrakis[2-(2',4'-difluorophenyl)-4-methylpyridine- C^2 , N']-bis(μ -chloro)diiridium(III) $[\text{Ir}(\text{F}_2\text{CH}_3\text{ppy})_2\text{Cl}]_2$. Yellow solid. Yield: 86% (2.19 g). *Anal. Calc.* for $\text{C}_{48}\text{H}_{32}\text{Cl}_2\text{F}_8\text{Ir}_2\text{N}_4$: C, 45.32; H, 2.54; N, 4.40. Found: C, 46.12; H, 2.44; N, 4.46%.

4.5.2. Dimer iridium complex **5**

Tetrakis[2-(2',4'-difluorophenyl)-3'-trifluoromethylphenyl)-4-methylpyridine- C^2 , N']-bis(μ -chloro)diiridium(III) $[\text{Ir}(\text{F}_2\text{CF}_3\text{CH}_3\text{ppy})_2\text{Cl}]_2$. Yellow solid. Yield: 79% (2.41 g). *Anal. Calc.* for $\text{C}_{52}\text{H}_{28}\text{Cl}_2\text{F}_{20}\text{Ir}_2\text{N}_4$: C, 40.45; H, 1.83; N, 3.63. Found: C, 41.12; H, 1.72; N, 3.68%.

4.5.3. Iridium(III)bis[2-(2',4'-difluorophenyl)-4-methylpyridinato- N, C^2]picolinate *N*-oxide, $(\text{F}_2\text{CH}_3\text{ppy})_2\text{Ir}(\text{pic-N-oxide})$ (**6**)

Yellow solid. Yield: 46%. (340 mg). $^1\text{H NMR}$ (300 MHz, CDCl_3 , ppm): 8.55 (d, 1H, $J = 5.7$ Hz), 8.32 (d, 1H, $J = 7.5$ Hz), 8.10 (s, 1H), 8.04 (s, 1H), 7.93 (td, 1H, $J = 1.5, 7.5$ Hz), 7.77 (d, 1H, $J = 5.4$ Hz), 7.38–7.43 (m, 1H), 7.24 (d, 1H, $J = 6.3$ Hz), 7.00 (dd, 1H, $J = 1.2, 5.7$ Hz), 6.78 (dd, 1H, $J = 1.2, 5.7$ Hz), 6.34–6.50 (m, 2H), 5.85 (dd, 1H, $J = 2.4, 8.7$ Hz), 5.59 (dd, 1H, $J = 2.4, 8.7$ Hz), 2.55 (s, 6H). *Anal. Calc.* for $\text{C}_{30}\text{H}_{20}\text{F}_4\text{IrN}_3\text{O}_3$: C, 48.78; H, 2.72; N, 5.69. Found: C, 48.58; H, 2.91; N, 5.29%.

4.5.4. Iridium(III)bis[2-(2',4'-difluoro-3'-trifluoromethylphenyl)-4-methylpyridinato- N, C^2]picolinate *N*-oxide, $(\text{F}_2\text{CF}_3\text{CH}_3\text{ppy})_2\text{Ir}(\text{pic-N-oxide})$ (**7**)

Yellow solid. Yield: 34% (297 mg). $^1\text{H NMR}$ (300 MHz, CDCl_3 , ppm): 8.57 (d, 1H, $J = 6.0$ Hz), 8.35 (d, 1H, $J = 7.2$ Hz), 8.18 (s, 1H), 8.13 (s, 1H), 8.00 (td, 1H, $J = 1.5,$

7.8 Hz), 7.76 (d, 1H, $J = 4.5$ Hz), 7.49 (t, 1H, 5.7 Hz), 7.12 (d, 1H, $J = 6.0$ Hz), 6.90 (d, 1H, $J = 6.3$ Hz), 5.64 (d, 1H, $J = 10.2$ Hz), 5.69 (d, 1H, $J = 10.8$), 2.59 (s, 6H). *Anal. Calc.* for $C_{32}H_{18}F_{10}IrN_3O_3$: C, 43.94; H, 2.07; N, 4.80. Found: C, 44.18; H, 2.35; N, 4.57%.

4.6. Measurements of physical and electrochemical properties

UV–visible absorption spectra of **6** and **7** were recorded by using a Varian 5000 spectrophotometer. Photoluminescence (PL) spectra were measured with a He:Cd laser (λ : 325 nm, and continuous wave) as the excitation light source and a photomultiplier tube (PMT, Hamamatsu) with a monochromator (Acton Research Co., SpectraPro 2300i) as the detector. Cyclic voltammograms (CV) of the Ir(III) complexes were recorded by using a Princeton Applied Research (AMETEK VSP) potentiostat at room temperature on 0.1 M solutions of the Ir(III) complexes in acetonitrile or dichloromethane containing tetrabutylammonium perchlorate (Bu_4NClO_4) at a scan rate of 100 mV/s under nitrogen gas. Pt was used as the working and counter electrode and Ag/AgCl electrode as the reference electrode.

The PL efficiencies of doped films containing **6** and **7** were measured using the integrating sphere (Newport) with a He:Cd laser (λ : 325 nm, and continuous wave) as the excitation light source. The absolute PL efficiency measurement system was calibrated by using two standard lamps of LS-1-CAL calibrated light source and DH-2000 deuterium–tungsten halogen light source (Ocean Optics, Inc.). Transient photoluminescence of the phosphorescent dye doped films were measured using a Nd:YAG laser (λ : 355 nm, 10 Hz, and 9 ns pulse width) as the excitation light source and PMT (Hamamatsu) with a monochromator (Acton Research Co., SpectraPro 2300i) as the detector. The samples were kept in a vacuum chamber maintained at pressures under 10^{-3} Torr during the measurement.

4.7. Fabrication of the PhOLEDs using Ir(III) complexes **6** and **7**

The PhOLEDs were fabricated by using thermal evaporation onto a cleaned glass substrate precoated with indium tin oxide (ITO) under a vacuum. Prior to organic layer deposition, the ITO substrates were exposed to UV–ozone flux for 10 min following degreasing in acetone and isopropyl alcohol. All of the organic layers were deposited by using thermal evaporation at a base pressure of $<5 \times 10^{-8}$ Torr. Current density–voltage–luminescence (J – V – L) characteristics of the PhOLEDs were measured simultaneously using a Keithley 2400 programmable source meter and Spectra-Scan PR650 (Photo Research). All the materials were purified using train sublimation before use.

Acknowledgement

This research was supported by a grant (2009K000069) from Center for Nanoscale Mechatronics and Manufacturing, one of the 21st Century Frontier Research Programs, which are supported by Ministry of Education, Science and Technology. This work was supported by the Korea Science and Engineering Foundation (KOSEF) grant funded by

the Korea government (MEST) (No. M10600000157-06J0000-15710) and Strategic Technology under Ministry of Knowledge Economy of Korea.

Appendix A. Supplementary data

Supplementary data associated with this article can be found, in the online version, at doi:10.1016/j.orgel.2009.12.014.

References

- [1] C.W. Tang, S.A. Van Slyke, *Appl. Phys. Lett.* 51 (1987) 913.
- [2] R.H. Friend, R.W. Gymer, A.B. Holmes, J.H. Burroughes, R.N. Marks, C. Taliani, D.D.C. Bradley, D.A. Dos Santos, J.L. Bredas, M. Logdlund, W.R. Salaneck, *W.R. Nature (London)* 397 (1999) 121.
- [3] R.J. Tseng, R.C. Chiechi, F. Wudl, Y. Yang, *Appl. Phys. Lett.* 88 (2006) 093512.
- [4] B.W. D'Andrade, S.R. Forrest, *Adv. Mater.* 16 (2004) 1585.
- [5] S. Lamansky, P. Djurovich, D. Murphy, F. Abdel-Razzaq, H.E. Lee, C. Adachi, P.E. Burrows, S.R. Forrest, M.E. Thompson, *J. Am. Chem. Soc.* 123 (2001) 4304.
- [6] W. Zhu, Y. Mo, M. Yuan, W. Yang, Y. Cao, *Appl. Phys. Lett.* 80 (2002) 2045.
- [7] X. Gong, J.C. Ostrowski, G.C. Bazan, D. Moses, A.J. Heeger, *Appl. Phys. Lett.* 81 (2002) 3711.
- [8] K.R.J. Thomas, M. Velusamy, J.T. Lin, C.H. Chien, Y.T. Tao, Y.S. Wen, Y.H. Hu, P.T. Chou, *Inorg. Chem.* 44 (2005) 5677.
- [9] W. Lu, B.X. Mi, M.C.W. Chan, Z. Hui, C.M. Che, N. Zhu, S.T. Lee, *J. Am. Chem. Soc.* 126 (2004) 4958.
- [10] C.H. Huang, F.Y. Li, W. Huang, *Introduction to Organic Light-Emitting Materials and Devices*, Fudan University, Shanghai, China, 2005.
- [11] M.A. Baldo, S. Lamansky, P.E. Burrows, M.E. Thompson, S.R. Forrest, *Appl. Phys. Lett.* 75 (1999) 4.
- [12] Y.S. Park, J.W. Kang, D.M. Kang, J.W. Park, Y.H. Kim, S.K. Kwon, J.J. Kim, *Adv. Mater.* 20 (2008) 1957.
- [13] D.M. Kang, J.W. Kang, J.W. Park, S.O. Jung, S.H. Lee, D. Park, Y.H. Kim, S.C. Shin, J.J. Kim, S.K. Kwon, *Adv. Mater.* 20 (2008) 2003.
- [14] K.S. Yook, S.O. Jeon, C.W. Joo, J.Y. Lee, *Appl. Phys. Lett.* 93 (2008) 113301.
- [15] J.J. Park, T.J. Park, W.S. Jeon, R. Pode, J. Jang, J.H. Kwon, E.S. Yu, M.Y. Chae, *Org. Electron.* 10 (2009) 189.
- [16] J. Lee, J.I. Lee, K.I. Song, S.J. Lee, H.Y. Chu, *Appl. Phys. Lett.* 92 (2008) 133304.
- [17] J. Brooks, Y. Babayan, S. Lamansky, P.I. Djurovich, I. Tsyba, R. Bau, M.E. Thompson, *Inorg. Chem.* 41 (2002) 3055.
- [18] P.C. Wu, J.K. Yu, Y.H. Song, Y. Chi, P.T. Chou, S.M. Peng, G.H. Lee, *Organometallics* 22 (2003) 4938.
- [19] D. Tanaka, Y. Agata, T. Takeda, S. Watanabe, J. Kido, *Jpn. J. Appl. Phys.* 46 (2007) L117.
- [20] S.J. Su, E. Gonmori, H. Sasabe, J. Kido, *Adv. Mater.* 20 (2008) 4189.
- [21] C. Yang, X. Zhang, H. You, L. Zhu, L. Chen, L. Zhu, Y. Tao, D. Ma, Z. Shuai, J. Qin, *Adv. Funct. Mater.* 17 (2007) 651.
- [22] K. Dedeian, J. Shi, N. Shepherd, E. Forsythe, D.C. Morton, *Inorg. Chem.* 44 (2005) 4445.
- [23] C.H. Yang, S.W. Li, Y. Chi, *Inorg. Chem.* 44 (2005) 7770.
- [24] P. Sajoto, P.I. Djurovich, A. Tamayo, M. Yousufuddin, R. Bau, M.E. Thompson, *Inorg. Chem.* 44 (2005) 7992.
- [25] H. Fukagawa, K. Watanabe, T. Tsuzuki, S. Tokito, *Appl. Phys. Lett.* 93 (2008) 133312.
- [26] Y. Zheng, S.H. Eom, N. Chopra, J. Lee, F. So, J. Xue, *Appl. Phys. Lett.* 89 (2008) 2343.
- [27] H. Jang, C.H. Shin, N.G. Kim, K.Y. Hwang, Y. Do, *Synth. Met.* 154 (2005) 157.
- [28] S.Y. Kim, J.H. Kim, Y. Ha, S.H. Lee, J.H. Seo, Y.K. Kim, *Curr. Appl. Phys.* 7 (2007) 380.
- [29] S.C. Lee, Y.S. Kim, *Mol. Cryst. Liq. Cryst.* 2491 (2008) 209.
- [30] V. Adamovich, J. Brooks, A. Tamayo, A.M. Alexander, P.I. Djurovich, B.W. D'Andrade, C. Adachi, S.R. Forrest, M.E. Thompson, *New J. Chem.* 26 (2002) 1171.
- [31] A.B. Tamayo, B.D. Alleyne, P.I. Djurovich, S. Lamansky, I. Tsyba, N.N. Ho, R. Bau, *J. Am. Chem. Soc.* 125 (2003) 7377.
- [32] P. Coppo, E.A. Plummer, L.D. Cola, *Chem. Commun.* 2004 (1774).
- [33] S.J. Yeh, M.F. Wu, C.T. Chen, Y.H. Song, Y. Chi, M.H. Ho, S.F. Hsu, C.H. Chen, *Adv. Mater.* 17 (2005) 285.

- [34] C.H. Yang, Y.M. Cheng, Y. Chi, C.J. Hsu, F.C. Fang, K.T. Wong, P.T. Chou, C.H. Chang, M.H. Tsai, C.C. Wu, *Angew. Chem. Int. Ed.* 46 (2007) 2418.
- [35] S.H. Kim, J. Jang, S.J. Lee, J.Y. Lee, *Thin Solid Films* 2517 (2008) 722.
- [36] N.G. Park, G.C. Choi, Y.H. Lee, Y.S. Kim, *Curr. Appl. Phys.* 6 (2006) 620.
- [37] L.L. Wu, C.H. Yang, I.W. Sun, S.Y. Chu, P.C. Kao, H.H. Huang, *Organometallics* 26 (2007) 2017.
- [38] H.J. Bolink, E. Coronado, S.G. Santamaria, M. Sessolo, N. Evans, C. Klein, E. Baranoff, K. Kalyanasundaram, M. Grätzel, M.D. Nazeeruddin, *Chem. Commun.* (2007) 3276.
- [39] P. Cippo, E.A. Plummer, L. De Cola, *Chem. Commun.* 2004 (1774).
- [40] T. Sajoto, P.I. Djurovich, A.B. Tamayo, M. Yousufuddin, R. Bau, M.E. Thompson, R.J. Holmes, S.R. Forrest, *Inorg. Chem.* 44 (2005) 7992.
- [41] Y. You, S.Y. Park, *J. Am. Chem. Soc.* 127 (2005) 12438.
- [42] P.I. Kvam, M.V. Puzyk, K.P. Balashev, J. Songstad, *Acta Chem. Scand.* (1995) 49.
- [43] K.P. Balashev, M.V. Puzyk, V.S. Kotlyar, M.V. Kulikova, *Coord. Chem. Rev.* 159 (1997) 109.
- [44] C. Hosokawa, H. Higashi, H. Nakamura, T. Kusumoto, *Synth. Met.* (1997) 91.
- [45] M. Matsuura, M. Funahashi, K. Fukuoka, H. Tokailin, C. Hosokawa, M. Edia, T. Kusumoto, *Proc. IDW'97* (1997) 581.
- [46] K.K.W. Lo, J.S.W. Chan, L.H. Lui, C.K. Chung, *Organometallics* 23 (2004) 3108.
- [47] C.L. Ho, W.Y. Wong, G.J. Zhou, Z. Xie, L. Wang, *Adv. Funct. Mater.* 17 (2007) 2925.
- [48] S.C. Lo, C.P. Shipley, R.N. Bera, R.E. Harding, A.R. Cowley, P.L. Burn, I.D.W. Samuel, *Chem. Mater.* 18 (2006) 5119.
- [49] P.J.J. Hay, *Phys. Chem. A* 106 (2002) 1634.
- [50] A.P. Wilde, K.A. King, R.J. Watts, *J. Phys. Chem.* 95 (1991) 629.
- [51] M.C. Columbo, A. Hauser, H.U. Güdel, *Top. Curr. Chem.* 171 (1994) 143.
- [52] Y. Wang, N. Herron, V.V. Grushin, D. LeCloux, V. Petrov, *Appl. Phys. Lett.* 79 (2001) 449.
- [53] F.O. Garces, K.A. King, R.J. Watts, *Inorg. Chem.* 27 (1998) 3464.
- [54] S. Reineke, K. Walzer, K. Leo, *Phys. Rev. B* 75 (2007) 125328.
- [55] N. Miyaura, A. Suzuki, *Chem. Rev.* 95 (1995) 2457.
- [56] S.Y. Takizawa, H. Echizen, J.I. Nishida, T. Tsuzuki, S. Yokito, Y. Yamashite, *Chem. Lett.* 35 (2006) 748.
- [57] M. Nonoyama, *Bull. Chem. Soc. Jpn.* 47 (1974) 767.